

## Modeling granule-based completely autotrophic nitrogen removal over the nitrite (CANON) process in an SBR

Qing Cai <sup>a,b,c,\*</sup>, Qiang He <sup>b</sup>, Sheng Zhang <sup>c</sup> and Jiajia Ding <sup>c</sup>

<sup>a</sup> Academic Affairs Office, Chongqing Vocational Institute of Engineering, Chongqing 402260, China

<sup>b</sup> College of Environment and Ecology, Chongqing University, Chongqing 400030, China

<sup>c</sup> Department of Environmental Planning, Chongqing Institute of Eco-Environmental Science, Chongqing 401147, China

\*Corresponding author. E-mail: qingcai85@cqvie.edu.cn

 QC, 0000-0002-2390-1325; QH, 0000-0001-8509-5608; SZ, 0000-0002-9115-0009; JD, 0000-0002-4344-6454

### ABSTRACT

Based on the simplified activated sludge model No. 1 (ASM1), a 1D biofilm model containing autotrophic and heterotrophic microorganisms was developed to describe the microbial population dynamics and reactor dynamics of completely autotrophic nitrogen removal over the nitrite in sequencing batch reactor (CANON SBR). After sensitivity analysis and calibration for parameters, the simulation results of  $\text{NH}_4^+$ -N concentration and  $\text{NO}_2^-$ -N concentration were consistent with the measured results, while the simulated  $\text{NO}_3^-$ -N concentration was slightly lower than the measured. The simulation results showed that the soluble microbial products had an extremely low concentration. The aerobic ammonia oxidation bacteria and anaerobic ammonia oxidation bacteria were the dominant microbial populations of the CANON system, while nitrite oxidization bacteria and heterotrophic bacteria were eliminated completely. The optimal ratio of air aeration load to influent  $\text{NH}_4^+$ -N load was about 0.18 L air/mgN. The operating condition of the reactor was optimized according to the simulation results, and the total nitrogen removal rate and the total nitrogen removal efficiency increased from  $0.312 \pm 0.015$  to  $0.485 \pm 0.013$  kg N/m<sup>3</sup>/d and from  $71.2 \pm 4.3$  to  $85.7 \pm 1.4\%$ , respectively.

**Key words:** Canon, granular sludge, heterotrophic bacteria, modeling, SBR

### HIGHLIGHTS

- The microbial population dynamics and the reactor dynamics model were developed.
- The model parameters were calibrated using the long-term operational data.
- The SMP had an extremely low concentration.
- The aerobic ammonia oxidation bacteria and anaerobic ammonia oxidation bacteria are dominant, while the nitrite oxidization bacteria are eliminated.

## 1. INTRODUCTION

The CANON process (Sliemers *et al.* 2002), in which partial nitrification and anaerobic ammonia oxidation (ANAMMOX) are implemented simultaneously, has been widely applied to full-scale wastewater treatment (Joss *et al.* 2011; Amin *et al.* 2021) since it can save 62.5% of O<sub>2</sub> consumption and 100% of organic carbon consumption theoretically compared to the traditional nitrification–denitrification process (Yao *et al.* 2013). The simultaneous growth of aerobic ammonia oxidation bacteria (AOB) and anaerobic ammonia oxidation bacteria (ANAOB) in the CANON process involves the competition on the common substrate  $\text{NH}_4^+$ , the synergy transformation of substrate  $\text{NO}_2^-$  and the different demands for the environmental conditions (especially for dissolved oxygen (DO)). There are both anaerobic and aerobic areas in granule-based biofilm, and thereby it is suitable for one-stage autotrophic nitrogen removal (Vangsgaard *et al.* 2013). The mathematical model provides an important means for profoundly investigating the mechanism and influencing factors of the CANON process (Abdelsalam 2018). The CANON biofilm model developed by Hao *et al.* (2002a, 2002b) revealed that the optimal DO level of maximum nitrogen removal was positively correlated with ammonia load (Hao *et al.* 2002b), and the positive and negative changes of DO by 0.2 gO<sub>2</sub>/m<sup>3</sup> have no significant impact on the performance of the CANON process (Hao *et al.* 2002a). Volcke *et al.*

This is an Open Access article distributed under the terms of the Creative Commons Attribution Licence (CC BY 4.0), which permits copying, adaptation and redistribution, provided the original work is properly cited (<http://creativecommons.org/licenses/by/4.0/>).

(2010) confirmed that the granular size affected the suitable DO concentration range of granular sludge, and the large granular sludge had a wider suitable DO concentration range. Vangsgaard *et al.* (2013) obtained the optimal operation load of the CANON system using the global sensitivity analysis method, namely,  $1.9 \text{ (gO}_2\text{/m}^3\text{/d)}/\text{(gN}_2\text{/m}^3\text{/d)}$ . A simplified biofilm model of the partial nitrification and anammox (PN/A) processes in SBR was developed recently to investigate the effects of anammox activity, DO concentration and fraction of inert biomass on performance. The simulation results showed that removing flocculent sludge is an effective strategy for the washout of NOB (Laureni *et al.* 2019). Wade & Wolkowicz (2021) demonstrate that the parameter space of the PN/A model can be partitioned into regions in which the system converges to different fixed points that represent different outcomes. Unfortunately, the simulation results have not been verified by experimental data.

Soluble microbial products (SMP) are organic compounds produced from the growth and decay of microorganisms. Researchers have gradually paid great attention to the heterotrophic microbial population using the SMP as growth substrate in autotrophic systems. A high level of heterotrophs existed in the autotrophic nitrifying biofilm system (Ni *et al.* 2011). Ni *et al.* (2011) simulated the influences of SMP on the growth of heterotrophic bacteria in the autotrophic nitrifying granular sludge system. They found that the heterotrophic bacteria that used SMP as growth substrate in the nitrifying granular sludge still took a certain proportion and could not be neglected; the anaerobic ammonia oxidation biofilm system also showed a similar situation (Ni *et al.* 2012). However, modeling of the influences of SMP on the heterotrophic microorganisms in the CANON system has not been carried out to our knowledge, which could be useful for a better understanding of the microbial population dynamics.

Based on the simplified activated sludge model No. 1 (ASM1) model (Henze *et al.* 1987), this study developed the microbial population dynamics and the reactor dynamics model for the granule-based CANON process containing autotrophic microorganisms, heterotrophic microorganisms and SMP. Moreover, the model parameters were calibrated by the long-term operational data. Subsequently, discussion was given to the microbial population dynamics and the influences of SMP on the heterotrophic microorganisms. Finally, to increase the capacity of the CANON SBR, the effects of air aeration rate and influent  $\text{NH}_4^+\text{-N}$  concentration that can be easily controlled by operators on performance were investigated, and the operating conditions were optimized with the developed model and verified by long-term operation. This study provided an alternative to improve the nitrogen removal of a CANON SBR.

## 2. MATERIALS AND METHODS

### 2.1. Experimental setup

An SBR with big height to diameter ratio was used to form the CANON granular sludge. The apparatus was a cylindrical vessel with a bore size of 14 cm and a working volume of 3 L. The reactor was inoculated with the sludge from another CANON SBR (Yao *et al.* 2013). The operating cycle was 240 min which consisted of 12 min aeration feeding, 150 min aeration reaction, 54 min stirring, 12 min settling and 12 min decanting period. The hydraulic retention time was 12 h. The details for the feeding substrate solution and trace element solution were described elsewhere (Yao *et al.* 2013). The DO concentration was kept at  $0.3 \pm 0.1 \text{ mg/L}$  by a gas flow meter at the aeration reaction stage, and the temperature was kept at  $31 \pm 1 \text{ }^\circ\text{C}$  by a water bath. The start-up experiments of the CANON SBR, which lasted for 160 days, were carried out to calibrate the model, and at the same time, the batch tests on the CANON sludge were conducted on day 34 and day 103 in SBR for model validation. And then the SBR operated continuously for 50 days on the optimal operating conditions to verify the simulated results. The influent and effluent  $\text{NH}_4^+\text{-N}$ ,  $\text{NO}_2^-\text{-N}$  and  $\text{NO}_3^-\text{-N}$  concentrations and the average volumetric granule size of sludge had been measured regularly.

### 2.2. Analytical methods

Mixed liquor suspended solids and mixed liquor volatile suspended solids,  $\text{NH}_4^+\text{-N}$ ,  $\text{NO}_2^-\text{-N}$  and  $\text{NO}_3^-\text{-N}$  concentrations were measured by the standard methods (APHA 1998). The DO concentration was measured with a DO electrode. The CANON granule size was determined using a laser diffraction particle size analysis instrument.

### 2.3. Model description

#### 2.3.1. Components, process stoichiometry and kinetics

A one-dimensional biofilm model based on the modified ASM1 has been performed in the Aquasim software (Reichert 1994) to simulate the microbial population dynamics and biological reactions (Supplementary Tables S1–S3) for the CANON process. The death-regeneration concept in ASM1 was used to describe the microbial decay. Seven solid species, including AOB ( $X_{\text{AOB}}$ ), NOB ( $X_{\text{NOB}}$ ), ANAOB ( $X_{\text{ANAOB}}$ ), active heterotrophic bacteria ( $X_{\text{H}}$ ), released slowly biodegradable substrate ( $X_{\text{S}}$ ), extracellular

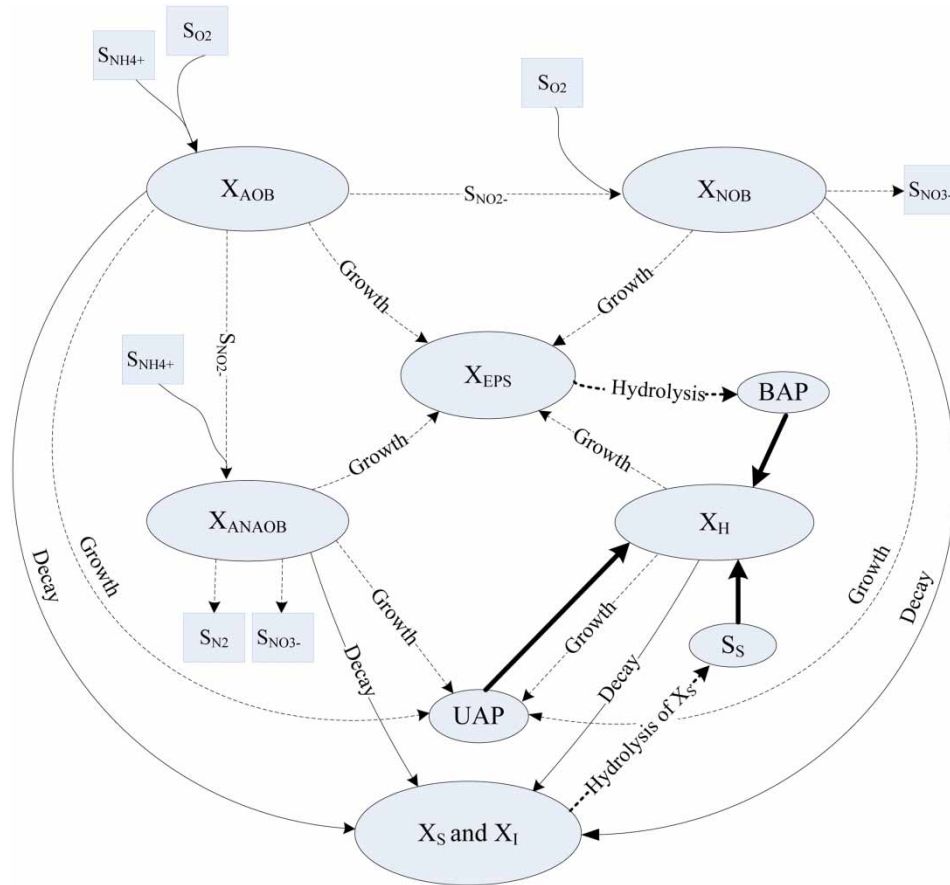


**Figure 1** | Schematic representation of microbial metabolic process in the CANON system.

polymeric substances ( $X_{EPS}$ ) and residual inert biomass ( $X_I$ ), and eight soluble species, including  $NH_4^+-N$  ( $S_{NH_4}$ ),  $NO_2^- -N$  ( $S_{NO_2}$ ),  $NO_3^- -N$  ( $S_{NO_3}$ ),  $DO$  ( $S_O$ ), dissolved  $N_2$  ( $S_{N_2}$ ), utilization-associated products ( $S_{UAP}$ ), biomass-associated products ( $S_{BAP}$ ) and hydrolyzed readily biodegradable substrate ( $S_S$ ), were taken into account (Figure 1). The growth of the ANAMMOX bacteria with  $NH_4^+-N$  and  $NO_2^- -N$  was described with Monod kinetics according to Ni *et al.* (2009). The heterotrophic growth on the SMP in CANON SBR is evaluated referring to the reported models in the nitrifying biofilm system (Ni *et al.* 2011) and the anammox biofilm system (Ni *et al.* 2012). It is assumed that organic carbon for the growth of the heterotrophic bacteria is produced by the growth of microorganisms (utilization-associated products, UAP), decay of biomass ( $X_S$  hydrolyzed to  $S_S$ ) and hydrolysis of EPS (biomass-associated products, BAP) (Ni *et al.* 2011). The stoichiometry and kinetic equations for AOB, NOB, ANAOB and the heterotrophic bacteria are listed in Supplementary Tables S1 and S2, and all the parameters in this model are defined in Supplementary Table S3.

### 2.3.2. Substrate diffusion

The mass transfer of  $O_2$  from gas phase to liquid phase in the model is expressed by the following equation (Mudliar *et al.* 2008):

$$r_{emt} = \frac{dS}{dt} = k_1 a (S_b - S_S) \quad (1)$$

where  $r_{emt}$  is the mass transfer rate;  $k_1 a$  is the mass transfer coefficient;  $S_b$  is the saturated substrate concentration;  $S_S$  is the substrate concentration. The oxygen mass transfer coefficient  $k_1 a_{O_2}$  involved in the model is linearly correlated with the gas

flow velocity of  $V_G$  in SBR, while the  $V_G$  is proportional to air aeration rate  $Q$  (Van Hulle *et al.* 2012):

$$k_l a_{O_2} = 0.6V_G = 0.6 \frac{Q}{A} \quad (2)$$

where  $A$  is the cross-sectional area of SBR.

The mass transfer resistance from liquid phase (bulk liquid) to solid phase (the surface of granular sludge) was ignored, and the internal mass transfer process of granular sludge can be in inference with the reports of Ni *et al.* (2009). Supplementary Table S3 shows the mass transfer coefficient of each substrate.

### 2.3.3. Initial conditions

The reactor volume was assumed to be fixed at 3 L. The granules size and their distribution could have an effect on the optimal range of DO concentration for the CANON process. The optimal range of DO concentration will be broader for large granules when influent  $\text{NH}_4^+$  concentrations increased (Volcke *et al.* 2010). Granules sludge grew from an initial radius of 0.1 mm to a steady state radius of 0.6 mm, which was the most typical for the particles in our lab-scale CANON SBR. The uniform particle size is adequate to be used to estimate the overall reactor performance (Volcke *et al.* 2012). The number of granular sludge was estimated according to the total effective sludge volume of CANON SBR and single granular sludge volume. The proportion of AOB, NOB, ANAOB and the heterotrophic bacteria was set as 5:5:6:20 initially, and they are assumed to uniformly distribute in the granule.

### 2.3.4. Sensitivity analysis and parameter calibration

The relative–absolute sensitivity equation in the AQUASIM software was selected to analyze the sensitivity of the parameters in the model:

$$\partial_{y,p}^{r,a} = \frac{1}{y} \frac{\partial y}{\partial p} \quad (3)$$

where  $\partial_{y,p}^{r,a}$  is the sensitivity analysis result,  $y$  is an arbitrary value (equal to the actual operational value) related to a model variable (e.g.,  $S_{\text{NH}_4}$  or  $X_{\text{AOB}}$ ), and  $p$  is a model parameter (e.g.,  $Y_{\text{AOB}}$  or  $\mu_{\text{AOB}}$ ). This equation calculates the absolute change of  $y$  with a 100% change in  $p$ . The sensitivity analysis gives a ranking of the averages of the absolute values for all model parameters (Ni *et al.* 2012), which is helpful to find out which are the parameters that have the greatest impact on the model components. The parameter calibration method was indicated as minimizing the residual sum of squares between the simulation results and measured results by changing parameter values. The parameters that were not calibrated in the model, such as the stoichiometry parameters, were all valued as those reported in references (Supplementary Table S3).

## 3. RESULTS AND DISCUSSION

### 3.1. Experimental observations

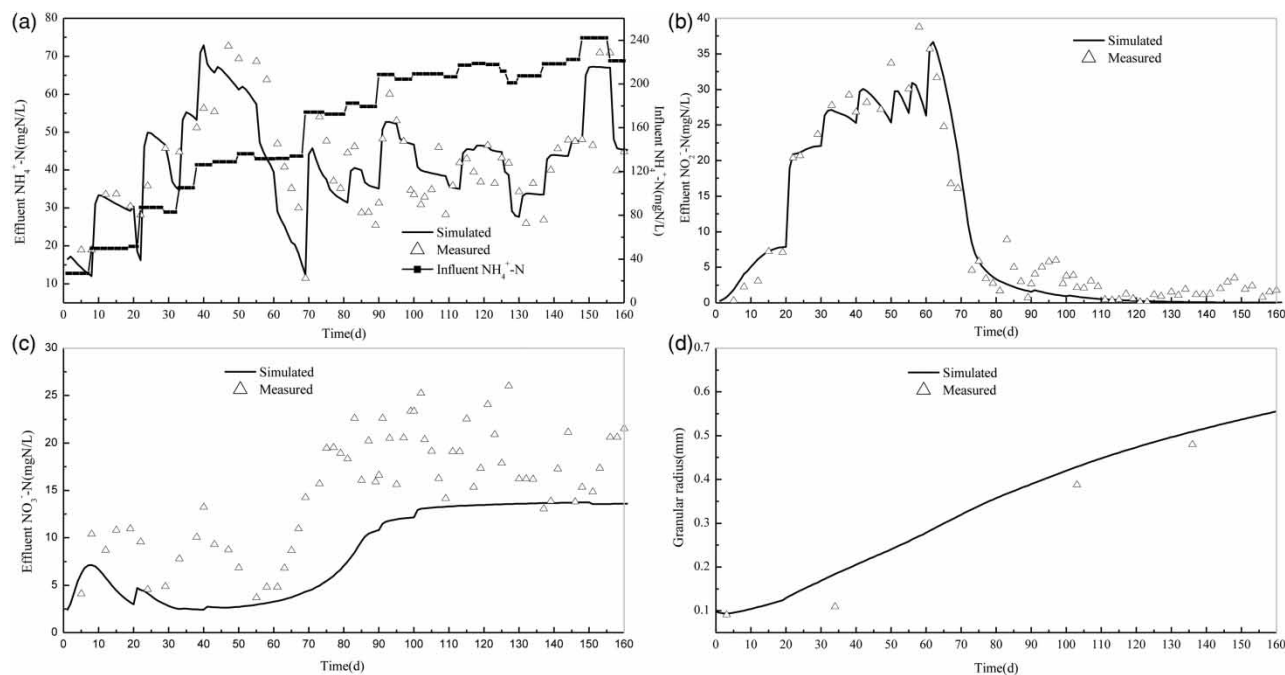
The SBR operated continuously for more than 200 days. The nitrogen loading rate increased from 0.054 to 0.557 gN/L/d though an increase in influent  $\text{NH}_4^+$ -N concentration from 26.9 to 278.7 mg/L. The total nitrogen removal efficiency gradually increased to 71.2% in the start-up experiments of 160 days and then finally reached up to 85.7% (Figure 7). Granular biomass (radius  $\geq 300 \mu\text{m}$ ) and floccular biomass (radius  $< 300 \mu\text{m}$ ) were both found in SBR, with a mean volumetric radius of about 0.6 mm.

### 3.2. Model calibration

The sensitivity analysis results of the model parameters are shown in Supplementary Table S4. The average relative–absolute sensitivity value of the yield coefficient for AOB ( $Y_{\text{AOB}}$ ) with respect to the  $\text{NH}_4^+$ -N concentration reached up to 10.69 mgN/L and exerted the maximum influences on the simulation results of  $\text{NH}_4^+$ -N concentration; the simulation results of  $\text{NO}_2^-$ -N concentration are most subject to the influences of the maximum growth rate of ANAOB ( $\mu_{\text{ANAOB}}$ ); the simulation results of  $\text{NO}_3^-$ -N concentration are mostly influenced by the yield coefficient for ANAOB ( $Y_{\text{ANAOB}}$ ). By comprehensively judging the influences of the parameters on the simulation results,  $Y_{\text{AOB}}$ ,  $\mu_{\text{AOB}}$ ,  $Y_{\text{ANAOB}}$  and  $\mu_{\text{ANAOB}}$  were selected to be calibrated.

**Table 1** | Calibration results for the parameters

Parameter	Calibration results	Results reported in references
$Y_{AOB}$ (g COD <sub>X</sub> /g N)	0.196	0.164 (Pambrun <i>et al.</i> 2006)
$\mu_{AOB}$ (/h)	0.0641	0.0583 (Moussa <i>et al.</i> 2005)
$Y_{ANAOb}$ (g COD <sub>X</sub> /g N)	0.29	0.21 (Ni <i>et al.</i> 2009)
$\mu_{ANAOb}$ (h <sup>-1</sup> )	0.0033	0.003 (Strous <i>et al.</i> 1998)

**Figure 2** | Model calibration with the effluent (a)  $\text{NH}_4^+\text{-N}$ , (b)  $\text{NO}_2^-\text{-N}$ , (c)  $\text{NO}_3^-\text{-N}$  concentrations and (d) granular radius in 160 days (dot for measurement and line for simulation).

The calibration results of these four parameters are presented in Table 1, which are both slightly higher than those reported in references (Strous *et al.* 1998; Moussa *et al.* 2005; Pambrun *et al.* 2006; Ni *et al.* 2009).

The profiles of the model predictions and experimental measurements for the effluent  $\text{NH}_4^+\text{-N}$  with the influent data, effluent  $\text{NO}_2^-\text{-N}$ ,  $\text{NO}_3^-\text{-N}$  and granular size in 160 days are shown in Figure 2(a)–2(d), respectively. As shown in Figure 2, the reactor was successfully started in 160 days with the formation of the CANON granules. The average absolute and relative errors of the simulated value and measured value of effluent  $\text{NH}_4^+\text{-N}$  concentration are 6.97 mgN/L and 18.03%, respectively, and the average absolute error of the simulated and measured  $\text{NO}_2^-\text{-N}$  concentrations is only 2.17 mgN/L. A good prediction was observed with respect to the effluent  $\text{NH}_4^+\text{-N}$  and  $\text{NO}_2^-\text{-N}$  concentrations and their disturbance, while the simulated effluent  $\text{NO}_3^-\text{-N}$  concentrations are generally lower than the measured values, with an average absolute error of 5.45 mgN/L and an average relative error of up to 35.18%. The NOB was completely eluted out after 50 days in the model (Figure 4), while the NOB were still found in actual granular and floccular biomass in CANON SBR (data not shown), which led to the effluent  $\text{NO}_3^-\text{-N}$  concentration of the model being lower than the measured value. The simulated granular size slightly exceeded the measured value in CANON SBR.

### 3.3. Model evaluation

To verify the reliability of the model, two groups of independent batch tests (data not used for model calibration) are conducted in the CANON SBR at the 34th (partial nitrification stage) and 103rd (completely autotrophic nitrogen removal stage) days, respectively, and the verification results are shown in Figure 3. As shown in Figure 3, the simulated  $\text{NH}_4^+\text{-N}$  and  $\text{NO}_2^-\text{-N}$

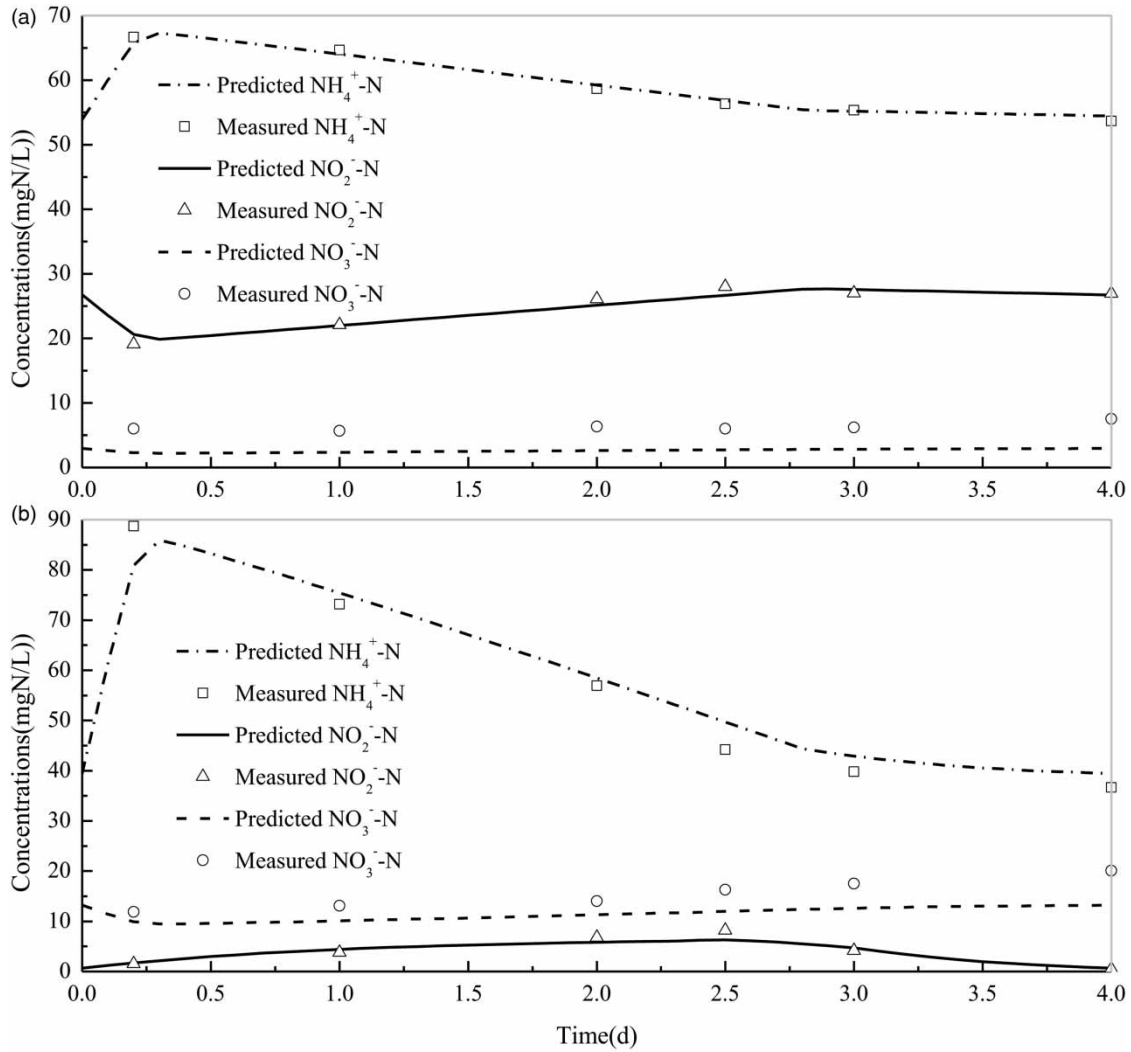


Figure 3 | Model verification with  $\text{NH}_4^+\text{-N}$ ,  $\text{NO}_2^-\text{-N}$ ,  $\text{NO}_3^-\text{-N}$  concentrations on (a) day 34 and (b) day 103.

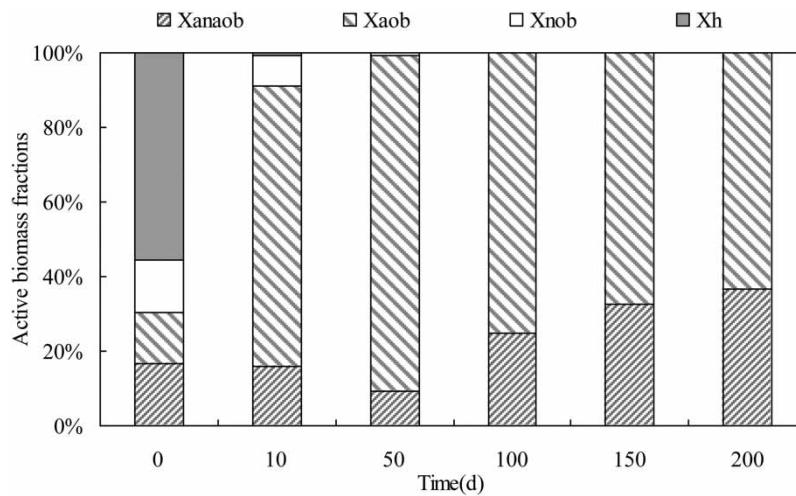


Figure 4 | Variation of active biomass fractions in CANON SBR.

concentrations in the 4 h typical operating cycle are consistent with the measured data; the average absolute error of  $\text{NH}_4^+\text{-N}$  concentration is merely 2.22 mgN/L, and the relative error is only 4.04%; the average absolute error of  $\text{NO}_2^-\text{-N}$  concentration is merely 0.76 mgN/L; the simulation results of  $\text{NO}_3^-\text{-N}$  concentration are slightly lower than the measured results.

### 3.4. Microbial population dynamics of the CANON process

The simulation results of microbial population dynamics were shown in Figure 4. As is shown, the AOB and ANAOB are the dominant microbial populations, while the NOB and heterotrophic bacteria are gradually eliminated. In the start-up process of CANON SBR, the relative content of AOB increased first and then decreased, while that of ANAOB decreased first and then increased; NOB and heterotrophic bacteria decreased gradually, and 50 days later, NOB and heterotrophic bacteria disappeared from the granular sludge.

The results of active biomass fractions distribution along the granule radius showed that AOB was mainly distributed at the outer layer of biofilm, while ANAOB at the inner layer after 100 days. The higher concentration of DO in the outer layer of biofilm was suitable for the growth of AOB, and the lower concentration of DO in the inner layer was suitable for the growth of ANAOB. Since the  $\text{O}_2$  affinity of AOB surpassed that of NOB (Joss *et al.* 2011) and took an advantageous position in the competition for  $\text{O}_2$ , as long as the substrate  $\text{NH}_4^+\text{-N}$  was not limited, NOB activity would be inhibited (Hawkins *et al.* 2010). In the case of oxygen-limited condition, the high  $\text{O}_2$  affinity of AOB could be used to remove NOB; meanwhile, limited by the mass transfer of DO, the NOB in the biofilm also took a disadvantageous position in the competition for the substrate  $\text{NO}_2^-\text{-N}$  with ANAOB, which resulted in the elimination of NOB. The heterotrophic bacteria were eliminated in the CANON system. This result was inconsistent with the reports in the autotrophic nitrifying granular sludge system (Ni *et al.* 2011) and the anaerobic ammonium oxidation granular sludge system (Ni *et al.* 2012). The heterotrophic bacteria using SMP as the growth substrate still occupied a large proportion (Ni *et al.* 2011, 2012) in the nitrifying granular sludge and the anaerobic ammonia oxidation granular sludge. Moreover, the growth of autotrophic bacteria directly affected the yield of SMP and the growth of heterotrophic bacteria (Ni *et al.* 2011, 2012). The simulation results showed that the SMP yielded by the growth and decay of microorganisms in the CANON system had an extremely low concentration (the sum of  $S_{\text{UAP}}$ ,  $S_{\text{BAP}}$ , and  $S_{\text{s}}$  concentration is lower than 1 mg COD/L). This is attributed to the fact that the DO limitation of the CANON system inhibited AOB growth. Meanwhile, the over-low  $\text{NO}_2^-$  concentration and incomplete anaerobic environment restricted the growth of ANAOB. The slow growth of autotrophic microorganism led to the SMP produced in the CANON system being far lower than that in the autotrophic nitrifying granular sludge system and the anaerobic ammonia oxidation granular sludge system. As a result, heterotrophic bacteria were eliminated.

### 3.5. Optimization of the operation strategy of CANON SBR

Using the simulation results at the 160th day as the initial condition, the influences of the influent  $\text{NH}_4^+\text{-N}$  concentration (200, 250 and 300 mgN/L) and the corresponding air aeration rate on the total nitrogen removal efficiency and the total nitrogen removal rate of CANON SBR were investigated with the developed model (Figure 5). The total nitrogen removal efficiency and the total nitrogen removal rate both increased first and then decreased with the increase of air aeration rate under different influent  $\text{NH}_4^+\text{-N}$  concentrations. When the influent  $\text{NH}_4^+\text{-N}$  concentration was 200 mgN/L and the aeration rate was 250 mL/min (the ratio of air aeration load to influent  $\text{NH}_4^+\text{-N}$  load kept at 0.187 L air/mgN), the total nitrogen removal efficiency reached up to 90.2% (Figure 5(a)). When influent  $\text{NH}_4^+\text{-N}$  concentration reached 250 mgN/L and the aeration rate was 300 mL/min (the ratio of air aeration load to influent  $\text{NH}_4^+\text{-N}$  load kept at 0.180 L air/mgN), the total nitrogen removal efficiency peaked at 91.8%. When the the influent  $\text{NH}_4^+\text{-N}$  concentration was 350 mgN/L and the aeration rate was 350 mL/min (the ratio of air aeration load to influent  $\text{NH}_4^+\text{-N}$  load kept at 0.175 L air/mgN), the total nitrogen removal efficiency reached 89.8%.

The relationship of the ratio of air aeration load to influent  $\text{NH}_4^+\text{-N}$  load with the total nitrogen removal efficiency is shown in Figure 6. It is clear that, at the ratio of air aeration load to influent  $\text{NH}_4^+\text{-N}$  load of about 0.18 L air/mgN, the total nitrogen removal efficiency of CANON SBR reached up to around 90%. The air aeration load in the CANON system directly affects the supply of DO. Since AOB's affinity to  $\text{O}_2$  is higher than that of NOB, the activity of NOB will be partially inhibited as long as  $\text{NH}_4^+\text{-N}$  is not limited (Hawkins *et al.* 2010). At the same time, DO reversibly inhibited the activity of ANAOB. As the DO concentration in CANON flocculent sludge exceeds 0.2 mg $\text{O}_2$ /L, anaerobic ammonia oxidation is inhibited (Joss *et al.* 2011).  $\text{NH}_4^+\text{-N}$  is the common substrate of AOB and ANAOB. Sufficient supply of  $\text{NH}_4^+\text{-N}$  can prevent AOB and ANAOB growth from being inhibited due to the lack of the substrate and effectively inhibit the growth of NOB (Hawkins *et al.* 2010). However, excess  $\text{NH}_4^+\text{-N}$  supply increases the effluent  $\text{NH}_4^+\text{-N}$  concentration of CANON system and thus influences the total nitrogen removal efficiency. Granular

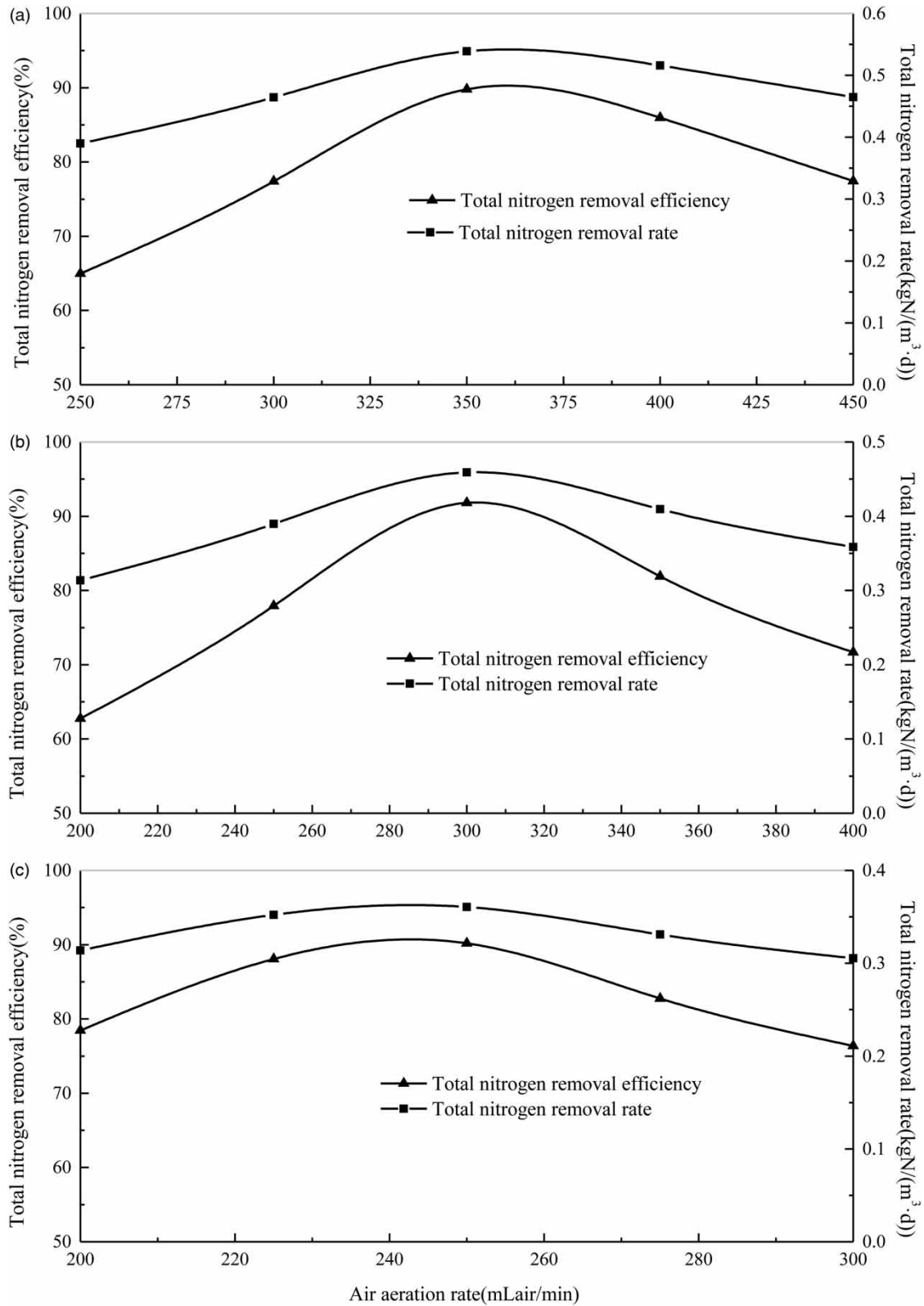


**Figure 5** | Performance of CANON SBR at different air aeration rates when influent  $\text{NH}_4^+\text{-N}$  concentration was (a) 200, (b) 250 and (c) 300 mgN/L, respectively.



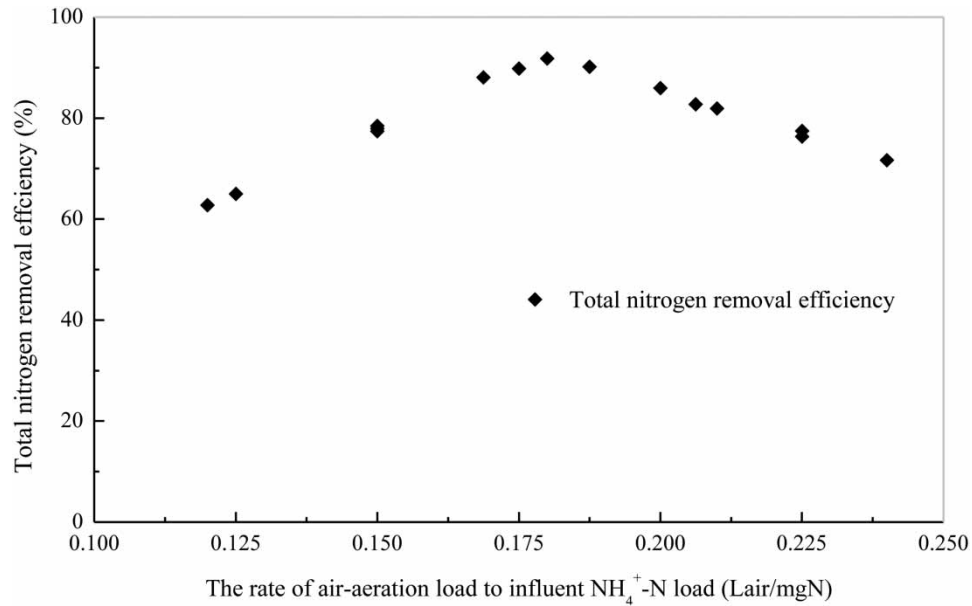


**Figure 6** | Total nitrogen removal efficiency at different ratios of air aeration load to influent  $\text{NH}_4^+\text{-N}$  load.

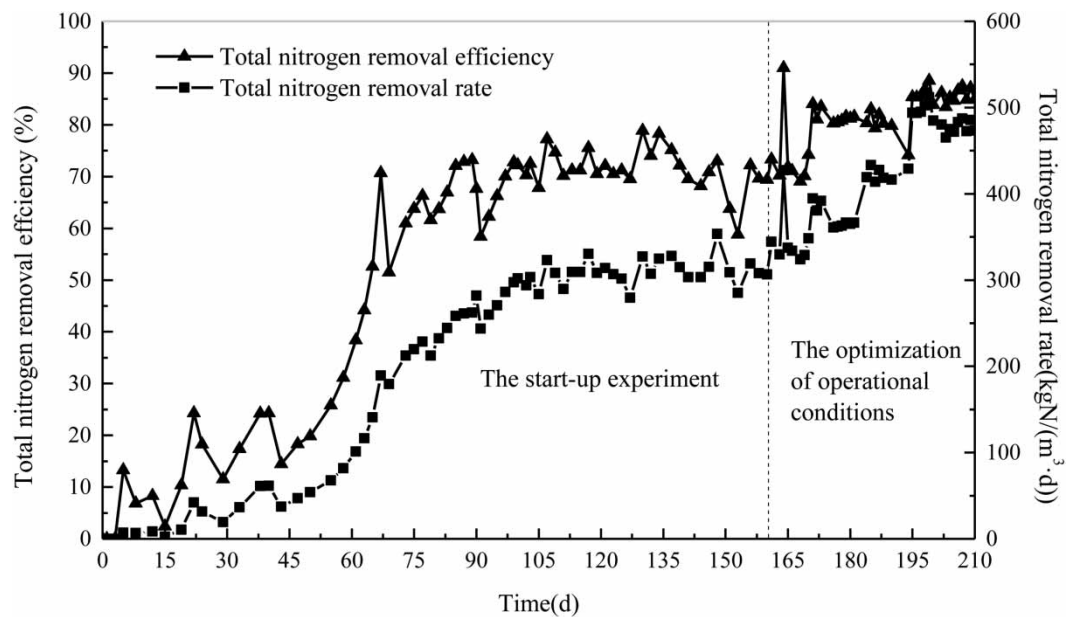


**Figure 7** | Performance of CANON SBR in the initial 160 days of operation and after the optimization of operational conditions.

size affects the mass transfer process of substrate. Granular sludge in large size adapts the DO and  $\text{NH}_4^+\text{-N}$  concentration in large range (Volcke *et al.* 2010). As for the sludge at certain granular size, the ratio of air aeration load to influent  $\text{NH}_4^+\text{-N}$  load maintains at a certain range, which increases the total nitrogen removal efficiency of CANON system. Simulation results showed that, when the ratio of air aeration load to influent  $\text{NH}_4^+\text{-N}$  load maintains at around 0.18 L air/mgN, the total nitrogen removal efficiency reaches to around 90% of the theoretical maximum in our CANON SBR.

In reference to the simulation results, the operation of the CANON SBR was optimized by keeping the ratio of air aeration load to influent  $\text{NH}_4^+\text{-N}$  load as 0.18 L air/mgN and increasing the influent  $\text{NH}_4^+\text{-N}$  concentration from 230 to 280 mgN/L gradually. The total nitrogen removal rate increased from  $0.312 \pm 0.015$  to  $0.485 \pm 0.013$  kg N/m<sup>3</sup>/d; meanwhile, the total nitrogen removal efficiency increased from  $71.2 \pm 4.3$  to  $85.7 \pm 1.4\%$  (Figure 7). The total nitrogen removal rate after

operating condition optimization exceeded those obtained by Sliemers *et al.* (2002) (0.3 kg N/m<sup>3</sup>/d) in the same type of reactor. Moreover, it is similar to that obtained by Vlaeminck *et al.* (2009) (0.5 kg N/m<sup>3</sup>/d), while lower than that obtained by De Clippeleir *et al.* (2009) (1.1 kg N/m<sup>3</sup>/d).

#### 4. CONCLUSIONS

1. Based on the simplified ASM1 model, a 1D biofilm model containing autotrophic microorganisms, heterotrophic microorganisms and SMP was developed to describe the microbial population dynamics and reactor dynamics of CANON SBR. After sensitivity analysis and calibration for parameters, the simulation results of NH<sub>4</sub><sup>+</sup>-N concentration and NO<sub>2</sub><sup>-</sup>-N concentration was consistent with the measured results, while the simulated NO<sub>3</sub><sup>-</sup>-N concentration was slightly lower than that measured due to the existence of a small amount of NOB in sludge.
2. Microbial population dynamics simulation results showed that, in the start-up process of CANON SBR, the relative content of AOB increased first and then decreased, while that of ANAOB decreased first and then increased; NOB and heterotrophic bacteria were eliminated gradually. The CANON system showed an extremely low SMP concentration, which resulted in the elimination of heterotrophic bacteria.
3. The reactor's dynamics simulation results suggested that the total nitrogen removal efficiency peaked at about 90% when the ratio of air aeration load to influent NH<sub>4</sub><sup>+</sup>-N load remained at about 0.18 L air/mgN. The operating condition was optimized according to the simulation results, and then the total nitrogen removal rate increased from 0.312 ± 0.015 to 0.485 ± 0.013 kg N/m<sup>3</sup>/d; meanwhile, the total nitrogen removal efficiency increased from 71.2 ± 4.3 to 85.7 ± 1.4%.

#### ACKNOWLEDGEMENTS

Funding from the Natural Science Foundation of China (No. NSF 51078365), Chongqing Special Postdoctoral Science Foundation (No. Xm2017175) and The Third Group of Young Backbone Teachers Funding Project from Chongqing Education Commission is gratefully acknowledged.

#### DATA AVAILABILITY STATEMENT

All relevant data are included in the paper or its Supplementary Information.

#### REFERENCES

- Abdelsalam, E. 2018 [Optimized biological nitrogen removal of high-strength ammonium wastewater by activated sludge modeling](#). *Journal of Water Reuse and Desalination* **8** (3), 393–403.
- Amin, M., John, L., Harsha, R., Akiyoshi, O., Noriatsu, O., Tomonori, K. & Hiroshi, A. 2021 [Treatment of landfill leachate with different techniques: an overview](#). *Journal of Water Reuse and Desalination* **11** (1), 66–96.
- APHA 1998 *Standard Methods for Examination of Water and Wastewater*, 20th edn. American Public Health Association, Washington, DC.
- De Clippeleir, H., Vlaeminck, S. E., Carballa, M. & Verstraete, W. 2009 [A low volumetric exchange ratio allows high autotrophic nitrogen removal in a sequencing batch reactor](#). *Bioresource Technology* **100** (21), 5010–5015.
- Hao, X. D., Heijnen, J. J. & Van Loosdrecht, M. C. M. 2002a [Model-based evaluation of temperature and inflow variations on a partial nitrification-ANAMMOX biofilm process](#). *Water Research* **36** (19), 4839–4849.
- Hao, X. D., Heijnen, J. J. & van Loosdrecht, M. C. M. 2002b [Sensitivity analysis of a biofilm model describing a one-stage completely autotrophic nitrogen removal \(CANON\) process](#). *Biotechnology and Bioengineering* **77** (3), 266–277.
- Hawkins, S., Robinson, K., Layton, A. & Saylor, G. 2010 [Limited impact of free ammonia on \*Nitrobacter\* spp. inhibition assessed by chemical and molecular techniques](#). *Bioresource Technology* **101** (12), 4513–4519.
- Henze, M., Grady, C., Gujer, W., Marais, G. & Matsuo, T. 1987 *Activated Sludge Model No. 1*. Scientific and Technical Reports No.1. London.
- Joss, A., Derlon, N., Cyprien, C., Burger, S., Szivak, I., Traber, J., Siegrist, H. & Morgenroth, E. 2011 [Combined nitrification-anammox: advances in understanding process stability](#). *Environmental Science & Technology* **45** (22), 9735–9742.
- Laurenti, M., Weissbrodt, D., Villez, K., Robin, O., Jonge, N., Rosenthal, A., Wells, G., Nielsen, J., Morgenroth, E. & Joss, A. 2019 [Biomass segregation between biofilm and flocs improves the control of nitrite-oxidizing bacteria in mainstream partial nitrification and anammox processes](#). *Water Research* **154**, 104–116.
- Moussa, M. S., Hooijmans, C. M., Lubberding, H. J., Gijzen, H. J. & van Loosdrecht, M. C. M. 2005 [Modelling nitrification, heterotrophic growth and predation in activated sludge](#). *Water Research* **39** (20), 5080–5098.

- Mudliar, S., Banerjee, S., Vaidya, A. & Devotta, S. 2008 Steady state model for evaluation of external and internal mass transfer effects in an immobilized biofilm. *Bioresource Technology* **99** (9), 3468–3474.
- Ni, B. J., Chen, Y. P., Liu, S. Y., Fang, F., Xie, W. M. & Yu, H. Q. 2009 Modeling a granule-based anaerobic ammonium oxidizing (ANAMMOX) process. *Biotechnology and Bioengineering* **103** (3), 490–499.
- Ni, B. J., Zeng, R. J., Fang, F., Xie, W. M., Xu, J. A., Sheng, G. P., Sun, Y. J. & Yu, H. Q. 2011 Evaluation on factors influencing the heterotrophic growth on the soluble microbial products of autotrophs. *Biotechnology and Bioengineering* **108** (4), 804–812.
- Ni, B. J., Rusalleda, M. & Smets, B. F. 2012 Evaluation on the microbial interactions of anaerobic ammonium oxidizers and heterotrophs in anammox biofilm. *Water Research* **46** (15), 4645–4652.
- Pambrun, V., Paul, E. & Sbrana, M. 2006 Modeling the partial nitrification in sequencing batch reactor for biomass adapted to high ammonia concentrations. *Biotechnology and Bioengineering* **95** (1), 120–131.
- Reichert, P. 1994 AQUASIM: a tool for simulation and data analysis of aquatic systems. *Water Science and Technology* **30** (2), 21–30.
- Sliekers, A. O., Derwort, N., Gomez, J. L. C., Strous, M., Kuenen, J. G. & Jetten, M. S. M. 2002 Completely autotrophic nitrogen removal over nitrite in one single reactor. *Water Research* **36** (10), 2475–2482.
- Strous, M., Heijnen, J. J., Kuenen, J. G. & Jetten, M. S. M. 1998 The sequencing batch reactor as a powerful tool for the study of slowly growing anaerobic ammonium-oxidizing microorganisms. *Applied Microbiology and Biotechnology* **50** (5), 589–596.
- Vangsgaard, A. K., Mutlu, A. G., Gernaey, K. V., Smets, B. F. & Sin, G. 2013 Calibration and validation of a model describing complete autotrophic nitrogen removal in a granular SBR system. *Journal of Chemical Technology & Biotechnology* **88**, 2007–2015.
- Van Hulle, S. W. H., Callens, J., Mampaey, K. E., van Loosdrecht, M. C. M. & Volcke, E. I. P. 2012 N<sub>2</sub>O and NO emissions during autotrophic nitrogen removal in a granular sludge reactor—a simulation study. *Environmental Technology* **1**, 1–10.
- Vlaeminck, S. E., Cloetens, L. F. F., Carballa, M., Boon, N. & Verstraete, W. 2009 Granular biomass capable of partial nitrification and anammox. *Water Science and Technology* **59** (3), 609–617.
- Volcke, E. I. P., Picioreanu, C., De Baets, B. & van Loosdrecht, M. C. M. 2010 Effect of granule size on autotrophic nitrogen removal in a granular sludge reactor. *Environmental Technology* **31** (11), 1271–1280.
- Volcke, E. I. P., Picioreanu, C., De Baets, B. & van Loosdrecht, M. C. M. 2012 The granule size distribution in an anammox-based granular sludge reactor affects the conversion—Implications for modeling. *Biotechnology and Bioengineering* **109** (7), 1629–1636.
- Wade, M. & Wolkowicz, G. 2021 Bifurcation analysis of an impulsive system describing partial nitrification and anammox in a hybrid reactor. *Environmental Science & Technology* **55** (3), 2099–2109.
- Yao, Z. B., Cai, Q., Zhang, D. J., Xiao, P. Y. & Lu, P. L. 2013 The enhancement of completely autotrophic nitrogen removal over nitrite (CANON) by N<sub>2</sub>H<sub>4</sub> addition. *Bioresource Technology* **146**, 591–596.

First received 1 June 2021; accepted in revised form 7 August 2021. Available online 24 August 2021